

THE INSTITUTE OF PAPER CHEMISTRY

Appleton, Wisconsin

Institute of Paper Science and Technology  
Central Files

END-LOAD COMPRESSION AND RELATED TOPICS

/ Project 1108-4

A Preliminary Report

to

TECHNICAL COMMITTEE  
FOURDRINIER KRAFT BOARD INSTITUTE, INC.

December 1, 1964

## TABLE OF CONTENTS

	Page
SUMMARY	1
INTRODUCTION	2
MACHINE-DIRECTION EDGEWISE COMPRESSION STRENGTH OF COMBINED BOARD	3
END-LOAD COMPRESSION FORMULA	8
RELATIONSHIP BETWEEN COMPONENT PROPERTIES AND EDGEWISE COMPRESSION OF COMBINED BOARD	10
LITERATURE CITED	19
APPENDIX. CONSIDERATION OF INELASTIC COLUMN BUCKLING	20

# THE INSTITUTE OF PAPER CHEMISTRY

Appleton, Wisconsin

## END-LOAD COMPRESSION AND RELATED TOPICS

### SUMMARY

Previous studies have indicated that end-to-end box compression strength is primarily dependent on the machine-direction edgewise compression strength  $P_{\underline{mx}}$  of the combined board. The methodology of evaluating  $P_{\underline{mx}}$  has been improved by using a harder wax, Carbowax 4000, as the agent for reinforcing the loading edges of a short column in place of Mobilwax D employed previously. On the average, column strengths were increased by 23% with the new method. There is evidence, however, that an even harder reinforcing agent may be needed for combined boards constructed with heavier grades of liner and for B-flute board.

The end-load compression formula was rederived using the improved estimates of  $P_{\underline{mx}}$ . This resulted in some adjustment in the empirical constants of the formula but no over-all improvement in accuracy was achieved. The accuracy of the formula is about 8%, on the average. Allied work is in progress to confirm the form of the end-load equation, particularly with respect to box dimensions.

In view of the importance of  $P_{\underline{mx}}$  to end-load compression, an analysis was made of the relationship of this property to component properties and combined board geometry. It was found that the combined board does not reach the edgewise compression strength of the liners in the machine direction. This result coincides with the observation that the combined board fails by buckling of the liners between flute tips. Interflute buckling of the liners depends upon their flexural stiffness ( $EI$ , e.g., Taber stiffness) and the distance between flute tips. A semi-empirical formula based on column buckling theory and involving Taber stiffness and distance between flute tips is shown to give reasonably good agreement with observed  $P_{\underline{mx}}$ , with an average accuracy of 9.4%. This result indicates that the

manufacturer of linerboard should be concerned primarily with the machine-direction Taber stiffness of the liner for end-to-end compression performance.

#### INTRODUCTION

The object of this study is to develop an equation relating end-to-end compression strength of RSC boxes to combined board and component properties and box dimensions. A preliminary equation was developed (1) involving (a) machine-direction edgewise compression strength of combined board, (b) flexural stiffness of the combined board in its principal directions, and (c) the length, width, and depth dimensions of the box. While the equation was in qualitative agreement with the major characteristics of end-load compression, it is believed that the accuracy (8-1/4%, on the average) can be improved upon. As discussed below, steps have been taken in an attempt to improve the accuracy. This involved improvement in the methodology of the edgewise compression test of combined board in the machine direction; this is the dominant material property in end-load compression. Consideration is also given to the component properties and combined board geometry governing edgewise compression in the machine direction of the combined board.

MACHINE-DIRECTION EDGEWISE COMPRESSION STRENGTH  
OF COMBINED BOARD

It appeared in earlier work that the methodology of the machine-direction edgewise compression test was not fully satisfactory, as evidenced by considerable rolling and bending of the loading edges despite their reinforcement with Mobilwax D paraffin. A number of harder formulations for edge reinforcement were screened, from which it appeared that Carbowax 4000 (melting point 200°F. approximately) offered real improvement. Subsequently, 52 samples from the original study were re-evaluated by the improved method, with the results shown in Table I and Fig. 1. The strengths tabulated are the averages for ten column specimens from a sample. The column dimensions were 4-1/2 flutes in the machine direction (load direction) by two inches wide. The loading edges were reinforced to a depth of one flute by dipping in molten wax.

It may be seen in Table I that the strength levels were markedly increased with Carbowax 4000 reinforcement relative to Mobilwax. On the average, the loads increased by 22.9%. Except for two samples, the differences ranged from essentially zero to 51.6%, with no evident trend depending on flute size or grade of board. The two exceptional samples were Samples 2324 and 2373, which exhibited significant decreases in load with Carbowax reinforcement - namely, -6.4 and -12.1%, respectively. Some of the board from the latter sample was subsequently found to have crushed flutes; this condition may affect the machine-direction column strength because of diminished lateral support given the liners by the crushed flutes. Accordingly, the results shown in Table I for this sample should be viewed with reservation. No reason was evident for the significant 6% decrease in the Carbowax specimens of Sample 2324. In the majority of samples, however, there was a marked increase in column strength through the use of Carbowax

TABLE I  
 EDGEWISE COMPRESSION STRENGTH OF COMBINED BOARD IN MACHINE DIRECTION  
 WITH TWO TYPES OF EDGE REINFORCEMENT

Sample No.	Series	Edgewise Compression, lb./in.			No. of Carbowax Specimens Exhibiting Edge Roll <sup>c</sup>
		Mobilwax D	Carbowax 4000	Difference, % <sup>a</sup>	
<u>A-Flute</u>					
1192	175	13.0	18.4	+41.5	0
1188	175	13.5	18.6	+37.8	0
2046	175	19.2	22.5	+17.2	0
1176	200	17.0	23.6	+38.8	1
1184	200	16.4	22.0	+34.1	0
2324	200	23.4 (20) <sup>b</sup>	21.9 (20)	- 6.4	0
1146	200	17.8	22.5	+26.4	0
1167	200	17.2	23.2	+34.9	0
1163	200	20.0	26.1	+30.5	0
2402	200	19.0	21.8	+14.7	0
2397	200	23.7	28.4	+19.8	0
2315	200	21.9	23.3	+ 6.4	0
2303	200	19.3	21.6	+11.9	0
2041	275	34.0	38.4	+12.9	0
2373	275	34.6 (26)	30.4 (27)	-12.1	1
2099	275	43.1	57.2	+32.7	3
2159	275	41.7 (20)	60.2 (5)	+44.4	2
2155	275	39.0	56.7	+45.4	0
				Av. +23.9	
<u>C-Flute</u>					
2219	175	20.6	24.3	+18.0	0
2211	200	20.2 (20)	20.0 (20)	- 1.4	0
2176	200	23.0	29.8	+29.6	0
2107	200	24.3	28.1	+15.6	1
2081	200	23.5	28.3	+20.4	0
2228	200	27.6	28.8	+ 4.3	0
2076	200	24.8	32.1 (9)	+29.4	0
2058	200	26.2	28.7	+ 9.5	0
2365	200	22.9	23.9	+ 4.4	1
2215	200	26.4 (20)	25.9 (20)	- 1.9	1
2145	200	23.1	30.8	+33.3	0
2171	200	23.6	33.5	+41.9	0
2398	200	22.9	34.7	+51.5	2
2150	200	23.6	26.0	+10.2	1
2090	200	23.8	26.5	+11.3	2
2094	200	21.8	25.0	+14.7	0
2111	275	40.6	47.4	+16.7	0
2141	275	47.0 (20)	57.6 (8)	+22.6	0
2369	275	41.8 (20)	51.0 (9)	+22.0	2
2033	275	38.9	52.8	+35.7	1
2050	275	41.9	56.3	+34.4	2
2103	275	40.6	44.3	+ 9.1	1
				Av. +19.6	
<u>B-Flute</u>					
2349	175	19.0	26.9	+41.6	2
2353	200	26.3	36.8	+39.9	1
2311	200	34.4 (20)	39.0	+13.4	5
2009	200	25.9	35.3	+36.3	0
2001	200	25.4	38.5	+51.6	0
2029	200	32.8	37.6	+14.6	3
2319	200	32.2 (20)	32.6 (20)	+ 1.2	2
2307	200	34.1	41.9	+22.9	4
2062	275	50.9 (20)	72.2	+41.8	0
2240	275	52.7	64.6	+22.6	3
2182	275	43.7 (20)	59.2	+35.5	2
2248	275	52.9	57.6	+ 8.9	5
				Av. +27.5	
				Composite av. +22.9	

<sup>a</sup> Difference, % based on values for Mobilwax D.

<sup>b</sup> Numeral in parentheses denotes number of specimens if other than 10.

<sup>c</sup> No. of specimens per sample of 10 Carbowax specimens.

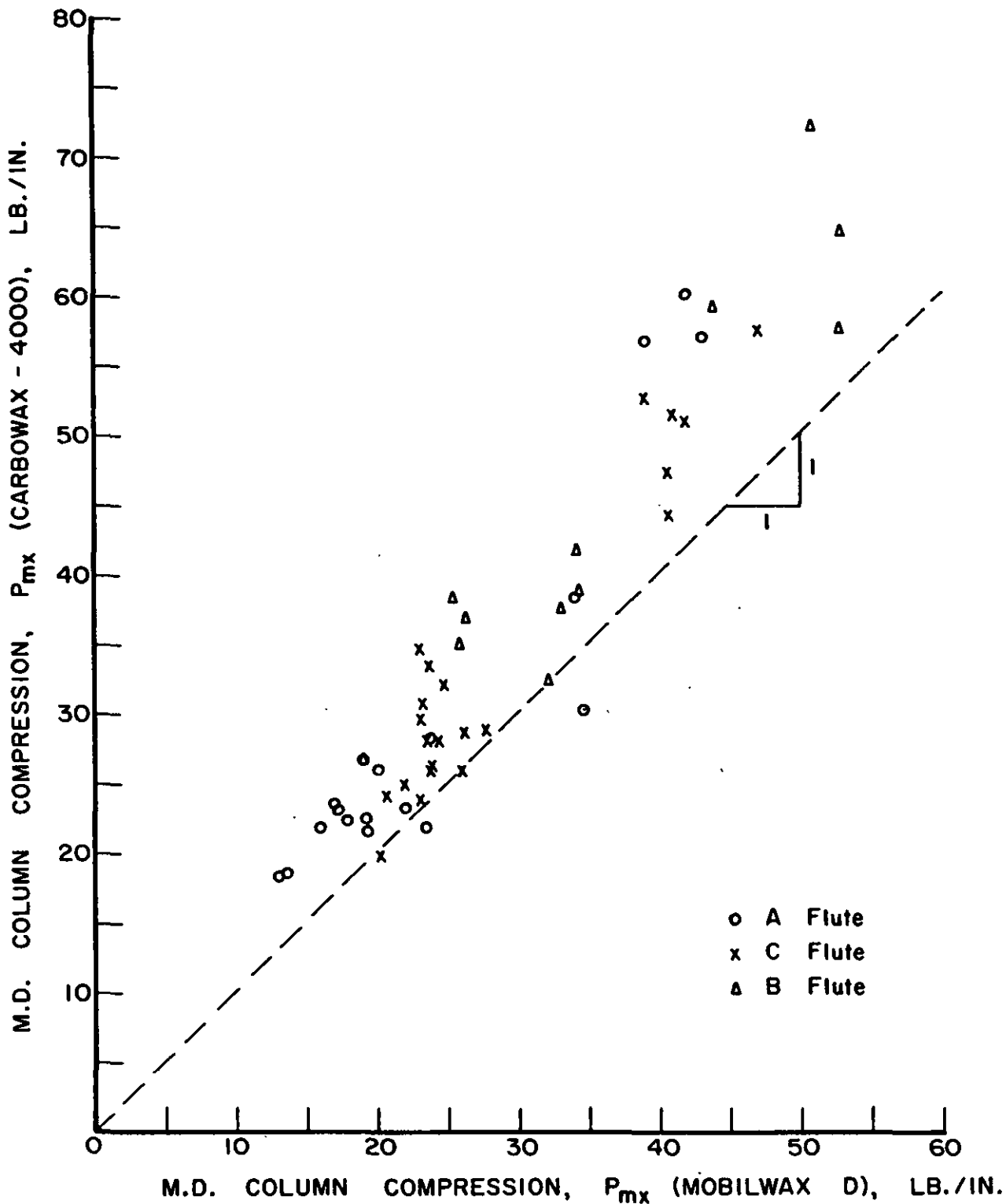


Figure 1. Relationship Between Loads of Machine-Direction Short Columns Reinforced with Carbowax 4000 and Mobilwax D

reinforcement. In compression testing, the magnitude of load is probably the best practical criterion for rating one test method against another, so that the superiority of Carbowax reinforcement is clear.

During the testing of the Carbowax reinforced columns the nature of failure of each specimen was observed. In general, the specimens failed between flute tips in the unreinforced portion of the specimen; this mode of failure is judged to be desirable and typical of machine-direction edgewise compression failure. Occasional rolling or bending of the reinforced edges did occur, however, as noted in the right-hand column of Table I; this mode of failure is judged to be undesirable.

The frequency of edge-rolled specimens in samples of size 10 is summarized in the following:

Number of Samples Exhibiting:

<u>No Edge Roll</u>	<u>1 roll</u>	<u>2 rolls</u>	<u>3 rolls</u>	<u>4 rolls</u>	<u>5 rolls</u>
29	9	8	3	1	2

It may be noted that the incidence of edge rolls increases with the sturdier combined board constructions, that is, heavier weight liners and/or small flute size. At first thought it may seem surprising that the incidence of edge roll is higher in boards with sturdier liners. It should be recognized, however, that edge roll is prevented by making the  $\underline{EI}$  of the wax-reinforced liner at an end of the specimen sufficiently greater than the  $\underline{EI}$  of the liner between flute tips to compensate for the lack of end-fixity of the former; it is a matter of the ratio of the two  $\underline{EI}$ 's. While a given type and amount of wax may be sufficient for a liner of low  $\underline{EI}$ , it may not offer a sufficiently high ratio for a liner of high  $\underline{EI}$ .

It is not clear at this time, however, whether the edge rolls can be definitely attributed to inefficient reinforcement or, on the other hand, to imperfections in cutting plane and parallel loading edges; the latter are known to adversely affect the machine-direction column test. Further study should be made of the sturdier combined constructions.

In summary, the harder reinforcement given by Carbowax 4000 markedly increased the machine-direction column load relative to Mobilwax D. On the basis of these results, Carbowax 4000 rather than Mobilwax D should be used for reinforcing machine-direction short columns. There is some indication that further improvement may be possible with sturdier combined board constructions (for example, B-flute and/or heavyweight liners) through the use of even stiffer reinforcing agents or possibly by improved cutting techniques.

### END-LOAD COMPRESSION FORMULA

In view of the marked increases in column strength discussed above, the numerical analysis leading to the end-load formula was performed again using the Carbowax column strengths in place of the previously used Mobilwax column strengths. In this case only 45 samples of boxes were available (rather than 57 samples as in the original study) because supplies of combined board of some samples were exhausted. Also, seven box samples with zero flap gap were omitted for reasons discussed in (1). The resulting equation is shown in Equation (1):

$$P = 0.26P_{mx} + 2.29P_{mx}^{0.785} \left( \sqrt{\frac{D_x D_y}{x y}} \right)^{0.214} (1 + W/L)^{0.754} W^{0.571} \quad (1)$$

as contrasted with the earlier formula, Equation (2):

$$P = 0.30P_{mx} + 3.10P_{mx}^{0.787} \left( \sqrt{\frac{D_x D_y}{x y}} \right)^{0.213} (1 + W/L)^{0.512} W^{0.574} \quad (2)$$

It may be seen that the numerical constants of the two equations are nearly the same. There is only a modest difference in the coefficients of the first term which represents the contribution of the side panels. The relative contributions of  $\frac{P_{mx}}{x}$ ,  $\sqrt{\frac{D_x D_y}{x y}}$  and  $W$  (all of which pertain to the flap panel) are virtually the same in both equations. The coefficient of the flap panel term decreased from 3.10 to 2.29; this is a change of 26% and probably mainly reflects the fact that the Carbowax column strength was higher than Mobilwax column strength by 23%, on the average.

The only change of substantial magnitude is in the exponent of the  $(1 + \frac{W}{L})$  factor which accounts for the effect of flap gap on end-load compression. This exponent increased from 0.512 to 0.754, with the interpretation that

somewhat greater importance is attached to the flap gap. This exponent is not determined very precisely, however, with this collection of samples. The 95% confidence interval on the exponent 0.754 is  $\pm 0.53$ . [In contrast, the exponent 0.785 on  $\frac{P}{\text{max}}$  is known ten times more precisely - namely, to within  $\pm 0.05$ .] Thus, the apparent difference in the exponents of  $(1 + \frac{W}{L})$  is not significant. It remains, however, that the effect of flap gap is not precisely determined in this mathematical model of end-load compression behavior.

The accuracy of the two equations is compared in Table II in terms of 43 samples of boxes which were common to both studies. It may be seen that the new equation improved the average accuracy only modestly - namely, from 8.6 to 8.2%. The distribution of differences within various ranges shows no over-all improvement with the new formula.

TABLE II

Equations	Average Diff., %	% Difference Within:					
		+5%	+10%	+15%	+20%	+25%	+30%
New [Equation (1)]	8.2	44	70	86	93	95	98 <sup>a</sup>
Old [Equation (2)]	8.6	30	60	91	98	98	100

<sup>a</sup>Maximum difference was 33%.

In summary, despite an improvement in the methodology of the machine-direction edgewise compression test, the accuracy of the end-load formula was not materially improved thereby. It is believed that further improvement in prediction of end-load compression strength should be directed to the functional make-up of the formula (relating to the underlying physical model of end-load compression). Work is in progress to confirm the effect of box dimensions on end-load compression.

RELATIONSHIP BETWEEN COMPONENT PROPERTIES AND EDGEWISE  
COMPRESSION OF COMBINED BOARD

Equations (1) and (2) reveal that the edgewise compression strength of the combined board is the dominant factor in end-to-end compression as in the case of top-to-bottom compression, although different directions of the board are involved in the two cases. It is important to control of quality in the mill and box plant to know which properties of the components govern machine-direction edgewise compression of the combined board,  $P_{\underline{\underline{mx}}}$ . It may be recalled that cross-direction edgewise compression of combined board (relating to top-to-bottom compression) is approximately equal to the sum of the modified ring compression of the component materials, accounting for medium draw, although more refined estimates take into consideration an effect of flute size (2).

Table III and Fig. 2 give a comparison of  $P_{\underline{\underline{mx}}}$  and the composite modified ring strength of the two liners in the machine direction. Modified ring strength of the corrugating medium is not included in this composite strength because the fluted medium is not in a configuration such that it can carry appreciable load in this direction and, moreover, the medium does not fail in the  $P_{\underline{\underline{mx}}}$  specimen. It may be seen that the composite ring strength of the two liners is greater than  $P_{\underline{\underline{mx}}}$  in all cases. On the average, composite ring compression strength is 59% greater than  $P_{\underline{\underline{mx}}}$ , with individual differences ranging from 10 to 132%. Two trends are evident in the data: (a) the difference between  $P_{\underline{\underline{mx}}}$  and composite ring strength is greatest for A-flute and least for B-flute (specifically, 86% for A-flute, 59% for C-flute, and 24% for B-flute); (b) the heavier the liner weight, the more nearly  $P_{\underline{\underline{mx}}}$  approaches the composite ring strength.

TABLE III  
 RELATIONSHIP BETWEEN MACHINE-DIRECTION EXEMISE COMPRESSION OF COMBINED  
 BOARD AND COMPONENT PROPERTIES

Sample No.	Series	Column Compression, P <sub>max</sub> , lb./in.	M.D. Modified Ring Compression, lb./in.			Machine Direction Taper Stiffness, D <sub>t</sub>	Flute Width, W, in.	D <sub>t</sub> /W <sup>2</sup>	Estimated P <sub>max</sub> [Eq. (4)]	Diff., % <sup>a</sup>
			Single Face	Double Face	Composite					
A-Flute										
1192	175	18.4	17.7	25.4	41.1	0.0557	0.1450	0.337	0.88	22.2
1188	175	18.6	17.5	22.4	39.9	0.0535	0.1091	0.337	0.72	20.0
2046	175	22.5	21.2	21.5	42.7	0.1018	0.1062	0.334	0.94	20.9
1176	200	23.6	23.3	22.9	46.2	0.1172	0.1253	0.339	1.06	24.3
1184	200	22.0	22.0	23.3	45.3	0.105.9	0.1187	0.338	1.06	24.4
1146	200	22.5	23.5	23.0	47.0	0.1377	0.1377	0.337	1.21	26.1
1167	200	23.2	23.2	23.0	46.2	0.1333	0.1245	0.337	1.14	25.2
1163	200	26.1	27.2	22.2	49.4	0.1760	0.1194	0.338	1.30	27.0
2397 & 2402	200	25.1	25.4	24.1	47.5	0.1289	0.1304	0.338	1.14	25.2
2315	200	23.3	24.2	22.5	46.7	0.1113	0.1062	0.336	0.96	23.2
2303	200	21.6	23.7	22.8	46.5	0.0938	0.0967	0.336	0.84	21.7
2099	275	57.2	34.9	36.7	71.6	0.4263	0.4454	0.338	3.81	46.2
2159	275	60.2	37.3	34.9	72.2	0.4263	0.4336	0.345	3.61	45.0
2155	275	56.7	27.2	40.8	68.0	0.1590	0.8468	0.346	4.19	48.5
Av. + 85.5										
C-Flute										
2219	175	24.3	21.8	20.4	42.2	0.1106	0.0960	0.338	0.91	22.5
2211	200	20.0	23.9	22.6	46.5	0.1004	0.0982	0.307	1.23	26.3
2176	200	29.8	24.9	28.2	53.1	0.1209	0.1941	0.307	1.68	30.7
2107	200	28.1	24.3	23.9	48.2	0.1487	0.1304	0.307	1.48	28.8
2281	200	28.3	22.7	23.0	45.7	0.1304	0.1194	0.307	1.32	27.2
2228	200	28.8	21.7	22.0	43.7	0.1355	0.1275	0.282	1.66	30.5
2076	200	32.1	24.7	22.9	47.6	0.1443	0.1443	0.307	1.36	27.6
2058	200	28.7	22.9	22.6	45.5	0.1626	0.1582	0.304	1.73	27.6
2365	200	23.9	22.1	21.8	43.9	0.1362	0.1399	0.284	1.72	31.0
2215	200	25.9	23.0	22.5	45.5	0.1033	0.0952	0.282	1.25	26.4
2145	200	30.8	23.4	23.4	46.8	0.1245	0.1048	0.308	1.21	26.0
2171	200	33.5	24.7	25.1	49.8	0.1318	0.1150	0.309	1.30	26.9
2398	200	34.7	24.3	24.3	48.6	0.1216	0.1260	0.284	1.53	29.3
2150	200	26.0	23.4	24.3	47.7	0.1187	0.1040	0.307	1.18	25.7
2090	200	26.5	24.6	23.6	48.2	0.0930	0.0945	0.311	0.97	23.3
2111	275	47.4	33.7	33.1	66.8	0.4996	0.4468	0.306	5.04	53.2
2141	275	57.6	35.1	36.0	71.1	0.4791	0.5318	0.309	5.30	54.5
2369	275	51.0	32.1	31.8	63.9	0.5069	0.4424	0.283	5.93	57.7
2033	275	52.8	33.3	33.3	66.6	0.3560	0.3545	0.287	4.31	49.2
2050	275	56.3	33.4	34.0	67.4	0.4761	0.4717	0.288	5.73	56.7
2103	275	44.3	35.6	34.9	70.5	0.4117	0.3624	0.284	4.93	52.6
Av. + 36.8										
B-Flute										
2349	175	26.9	21.1	19.0	40.1	0.0703	0.0615	0.237	1.17	25.6
2353	200	36.8	21.3	23.6	44.9	0.1275	0.1201	0.238	2.18	35.0
2009	200	35.3	23.2	23.1	46.3	0.1267	0.1296	0.238	2.26	35.5
2001	200	38.3	24.0	23.5	47.5	0.1253	0.1201	0.238	2.16	34.8
2029	200	37.6	24.2	22.2	46.4	0.1084	0.1128	0.239	1.93	32.9
2319	200	32.6	22.8	22.9	45.7	0.1011	0.1018	0.239	1.78	31.6
2062	275	72.2	39.4	40.3	79.7	0.5904	0.5611	0.239	10.06	75.2
2240	275	64.6	36.6	36.6	73.2	0.4791	0.4750	0.235	7.76	66.0
2182	275	59.2	31.4	35.8	67.2	0.3838	0.4248	0.239	7.09	63.1
2248	275	57.6	28.4	36.2	64.6	0.4175	0.4351	0.237	7.60	65.3
Av. + 23.9										
Composite av. + 59.3										

<sup>a</sup>Based on observed P<sub>max</sub>.

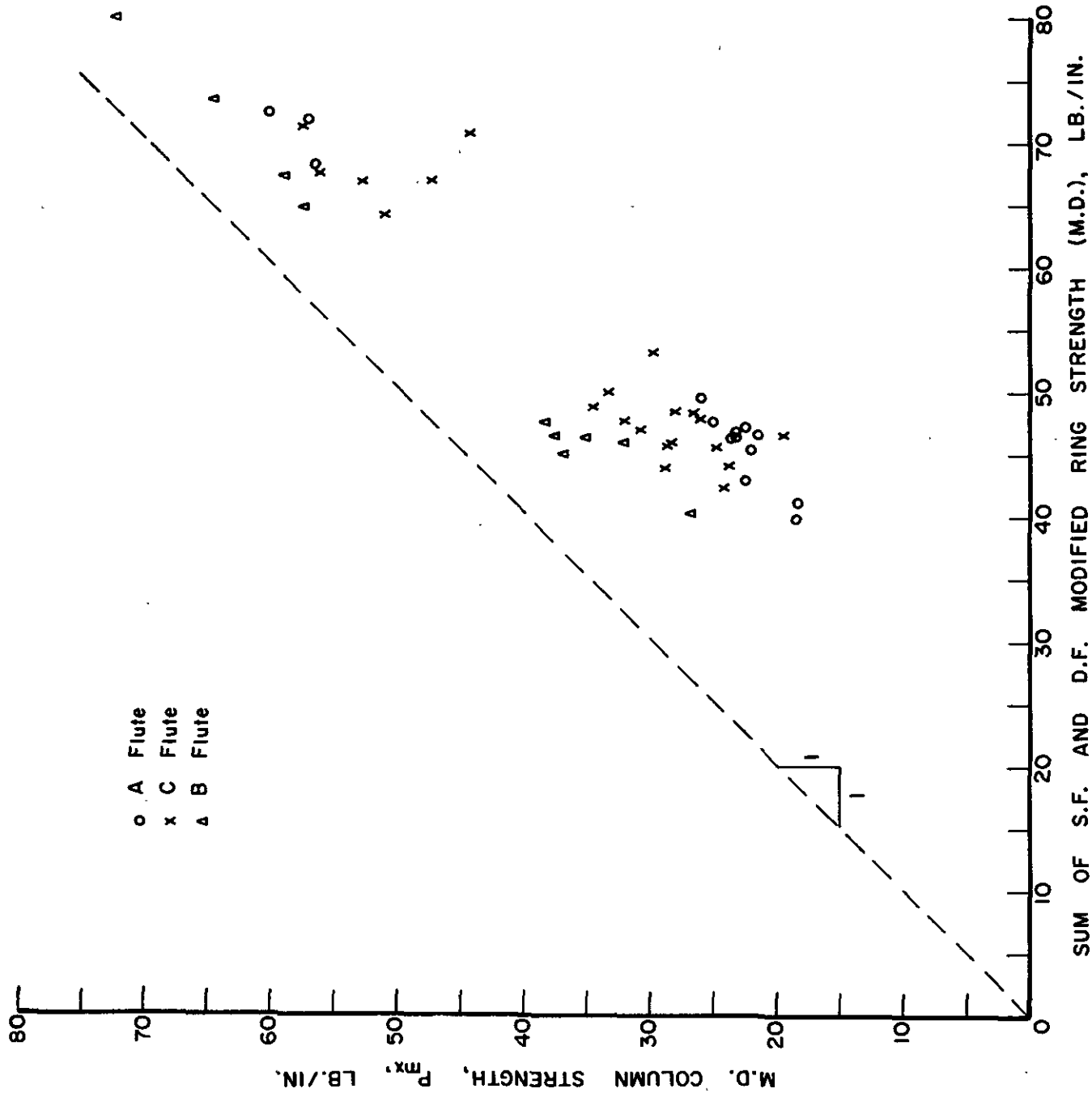


Figure 2. Relationship Between Machine-Direction Edgewise Compression Strength of Combined Board and Composite Modified Ring Compression of Liners

The above comparison of  $P_{\text{max}}$  and composite modified ring compression of the liners shows that the liners do not reach their edgewise compression strength when the combined board is compressed in the machine direction. Instead, each element of liner between flute tips apparently acts as an individual column that bends and buckles rather than crushes.

From consideration of column theory, the following two properties of the combined board and its components are of primary importance to interflute buckling of the liners. The first property of importance is the height of the element of liner between flute tips. B-flute board, for example, has a relatively short column height between flute tips and, therefore, has substantially higher machine-direction compression strength than A-flute board with the same components; this may be seen in general in Table III by comparing the several flute sizes in the same bursting strength series. For example, in the 200-lb. series boards, the average value of  $P_{\text{max}}$  is 23.4 lb./in. for A-flute, 28.3 lb./in. for C-flute and 36.2 lb./in. for B-flute. It may be recalled that end-load strengths of boxes constructed in these flute sizes are ranked in the same order.

The second property of importance to liner buckling between flute tips is the machine-direction flexural stiffness of the liner. Thus, in so far as component properties are concerned, Taber stiffness of the liners, rather than modified ring compression of the liners, may be expected to govern edgewise compression of the combined board in the machine direction.

It is believed that the corrugating medium has only a minor influence on the edgewise compression of combined board in the machine direction. The fluted medium probably carries negligible load and mainly serves to define the column height and end fixity of the liner elements between flute tips.

Column theory indicates that the degree of fixity of the liner element at the flute tips and the Poisson ratio for the liner also determine the buckling strength of the liner element (3). Neither of these factors is readily measurable at the present time and in the following analysis it will be assumed that they are constant for the several samples of combined board. With this approximation, column theory indicates that  $\underline{P}_{\underline{mx}}$  is related to liner properties and flute geometry by an equation of the following form:

$$P_{mx} = k D_x / W^2 \quad (3)$$

where

$\underline{P}_{\underline{mx}}$  = machine-direction edgewise compression strength of combined board, lb./in.

$\underline{D}_{\underline{x}}$  = average machine-direction Taber stiffness of liners, lb.-in.

$\underline{W}$  = distance between flute tips, in.

$\underline{k}$  = a constant reflecting average values of column end fixity and Poisson ratio

Table III shows  $\underline{P}_{\underline{mx}}$ ,  $\underline{D}_{\underline{x}}$  and  $\underline{W}$  for 45 samples of combined board available to this study. Figure 3 is a graph of  $\underline{P}_{\underline{mx}}$  vs.  $\underline{D}_{\underline{x}} / \underline{W}^2$ , the latter being the important parameter in liner buckling behavior. It may be seen that the entire collection of data points does not cluster closely about a single straight line, as would be expected from Equation (3). Only those 31 samples with  $\underline{D}_{\underline{x}} / \underline{W}^2$  less than about 2.5 show promise of fitting a straight line as indicated by Equation (3). These samples have, in general, lighter weight liners with low Taber stiffness. A straight line fitted to this selected group of samples was found to be  $\underline{P}_{\underline{mx}} = 11.13 \underline{D}_{\underline{x}} / \underline{W}^2 + 12.33$ . The average difference between observed and predicted  $\underline{P}_{\underline{mx}}$  based on this equation was 8.7%.

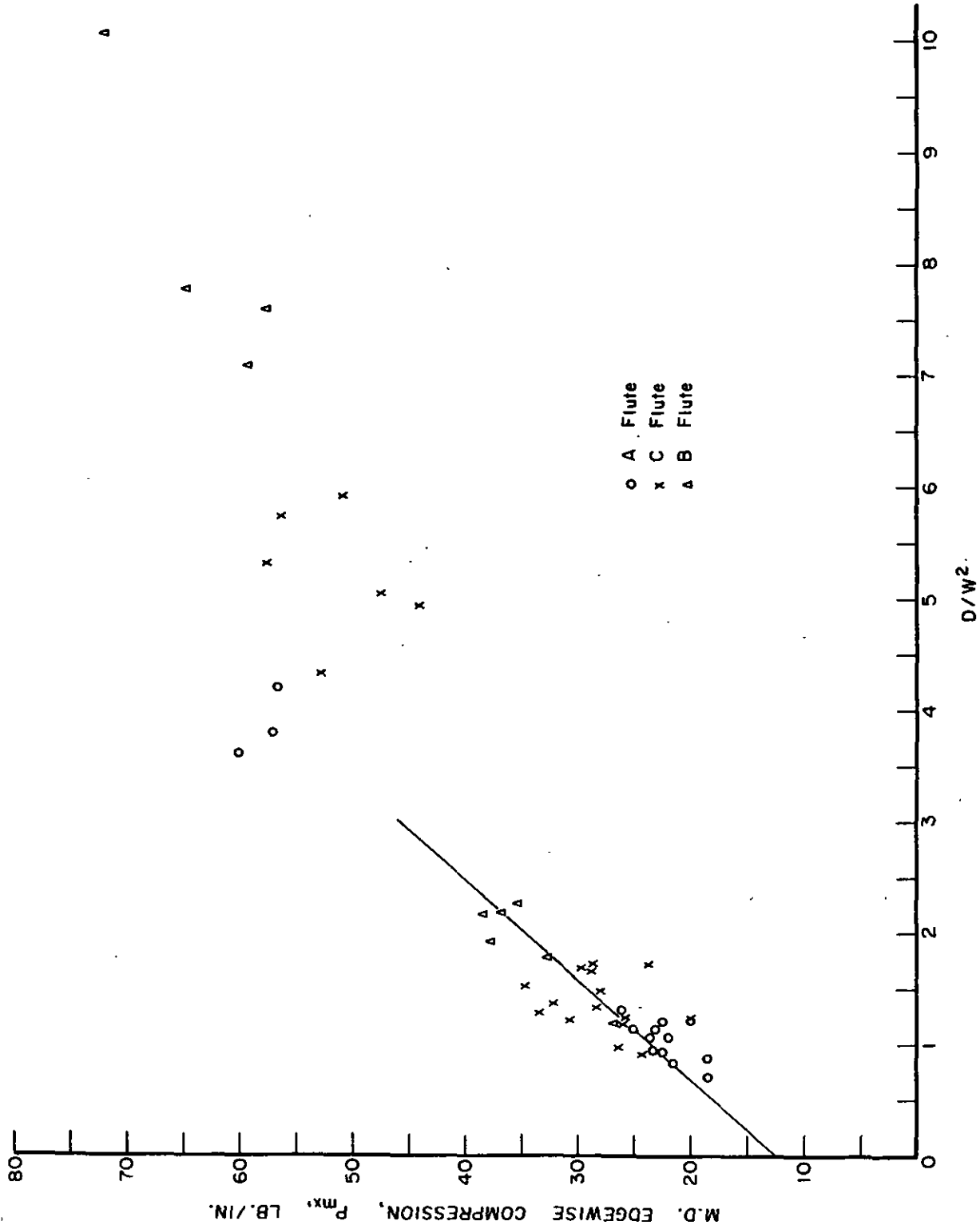


Figure 3. Relationship Between Machine-direction Edgewise Compression Strength of Combined Board ( $P_{max}$ ) and the Interflute Buckling Parameter of the Liner ( $D/W^2$ )

Consideration of all of the data plotted in Fig. 3 suggests that there is a curvilinear relationship between  $\frac{P_{\underline{mx}}}{\underline{x}}$  and  $\frac{D_{\underline{x}}}{W^2}$ . Moreover, there are theoretical grounds for expecting a curvilinear relationship. This latter consideration relates to the likelihood of inelastic buckling of the liners and is developed in the Appendix to this report. Briefly, the reasoning is as follows: As  $\frac{D_{\underline{x}}}{W^2}$  increases, corresponding to stiffer liners and/or smaller flute distance between tips, it is likely that the liner buckles inelastically, that is, at a stress level beyond the proportional limit of the stress-strain curve. For example, Table III or Fig. 2 reveals that some of the "sturdier" boards buckle at loads approaching the edgewise compression strength of the liners and hence are probably at a level beyond the proportional limit. For these samples, the Taber stiffness (EI) is not appropriate in the column formula. An inelastic modulus is required which is less than the modulus in Taber stiffness inasmuch as the latter is essentially an elastic property. Use of Taber stiffness in these instances overestimates the liner buckling strength. It is shown in the Appendix that if the detailed calculations were made to account for inelastic buckling of the liners, it would lead to a curvilinear relationship between  $\frac{P_{\underline{mx}}}{\underline{x}}$  and  $\frac{D_{\underline{x}}}{W^2}$ . Stated another way,  $\frac{D_{\underline{x}}}{W^2}$  as evaluated in this study overestimates the buckling strength and the plotted points for the sturdier liners (large  $\frac{D_{\underline{x}}}{W^2}$ ) lie too far to the right in Fig. 3. Therefore, if it is desired to employ Taber stiffness (the alternative involving inelastic modulus would become quite unwieldy), then the relationship between  $\frac{P_{\underline{mx}}}{\underline{x}}$  and  $\frac{D_{\underline{x}}}{W^2}$  should be curvilinear.

In view of the above, a power function was fitted to the entire collection of data. That a power function is appropriate is apparent from the log-log plot in Fig. 4, where it may be seen that the points suggest a straight line in

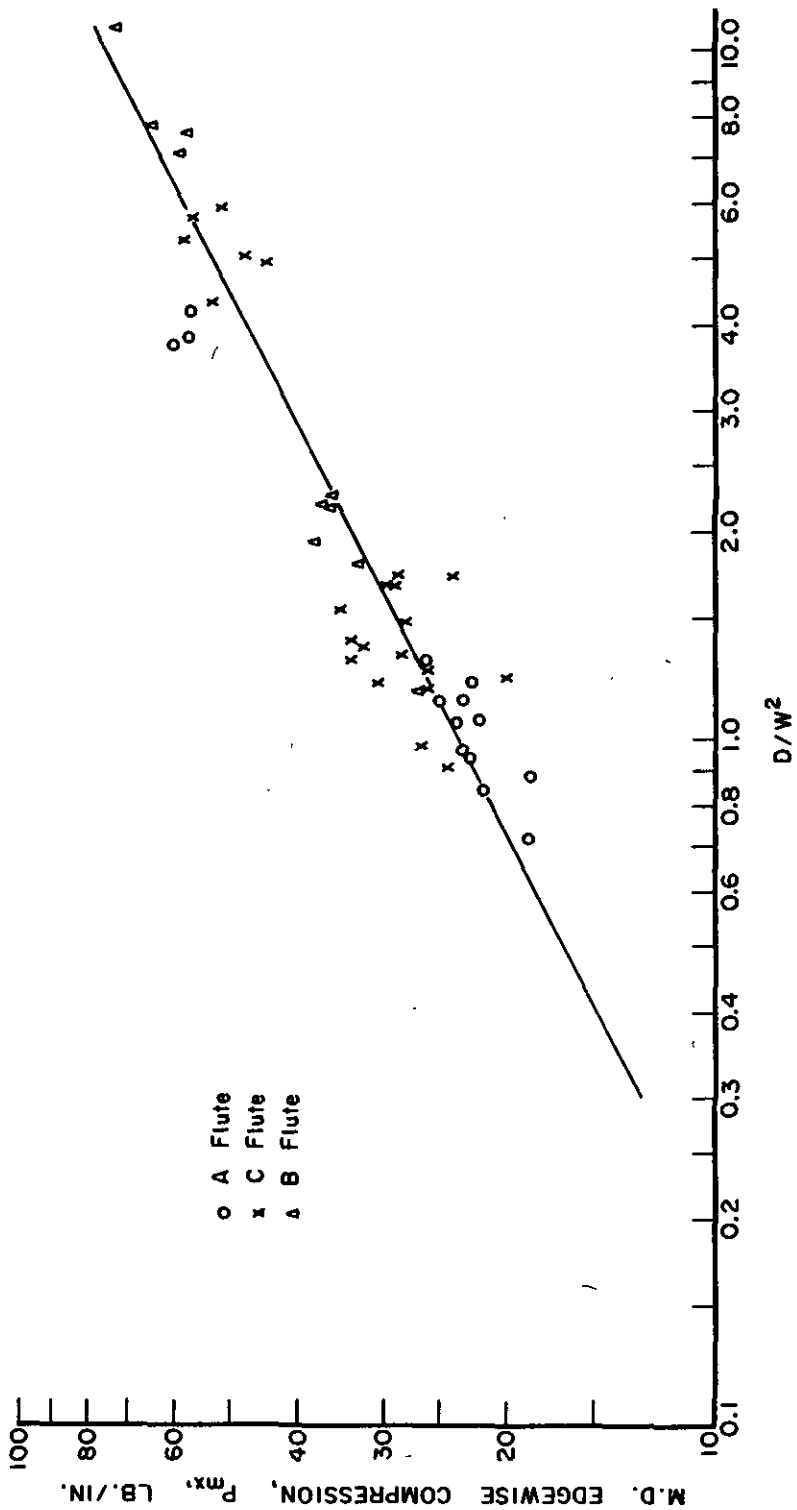


Figure 4. Relationship Between  $P_{mx}$  and  $D/W^2$  in Log-Log Co-ordinates

these co-ordinates and hence a power function in rectilinear co-ordinates. The power function of best fit was found to be:

$$P_{\text{mx}} = 23.67 (D_x/W^2)^{0.500} \quad (4)$$

With this equation the average difference between observed and predicted  $P_{\text{mx}}$  was 9.4% for the entire collection of samples. Individual sample differences are shown in Table III. The distribution of differences is given in Table IV.

TABLE IV  
 ACCURACY OF PREDICTED  $P_{\text{mx}}$   
 [Equation (4)]

% Differences Within:						Max.
+5%	+10%	+15%	+20%	+25%	+30%	Diff.
38	60	78	91	93	98	31.5%

Inspection of Fig. 4 reveals that there is still substantial variation in  $P_{\text{mx}}$  which is not accounted for by the liner buckling parameter  $D_x/W^2$ . Among the possible reasons for the residual errors are (a) lack of information on column end fixity and Poisson ratio of the liner elements, (b) variation in "washboarding" of single-face liner which is not accounted for in the interflute buckling consideration, and, in the case of the constructions of high  $D_x/W^2$ , (c) the approximate treatment of inelastic effects. Nonetheless, it appears that the essential behavior of combined board in machine-direction edgewise compression involves liner buckling between flute tips rather than edgewise crushing of the components. This result means that the manufacturer of linerboard should be concerned primarily with the Taber stiffness of the liner with respect to end-to-end box compression.

LITERATURE CITED

1. The Institute of Paper Chemistry. End-load compression. A preliminary report to the Technical Committee. Project 1108-4, August 20, 1963.
2. The Institute of Paper Chemistry. Relationship between the edgewise compression strength of combined board and component properties. A preliminary report to the Technical Committee. Project 1108-4, July 18, 1963.
3. Houbolt, J. C., and Stowell, E. Z. Critical stress of plate columns. Washington, D. C., National Advisory Committee for Aeronautics. Technical Note 2163, Aug., 1950.
4. Timoshenko, S. P., and Gere, J. M. Theory of elastic stability. p. 178. New York, McGraw-Hill Book Co., 1961.

APPENDIX

CONSIDERATION OF INELASTIC COLUMN BUCKLING

The buckling load  $\underline{P}_{cr}$  (load per unit width) of a wide column of length  $\underline{W}$  for which the stress is in the inelastic range is given by (4):

$$P_{cr} = \frac{K E_t I}{W^2} \quad (5)$$

where  $\underline{E}_t$  is the slope of the tangent to the stress-strain curve at the stress level corresponding to the buckling load;  $\underline{I}$  is the moment of inertia of the column cross section per unit width; and  $\underline{K}$  is a function of end fixity and Poisson's ratio. Equation (5) may be rewritten as follows:

$$P_{cr} = K \eta \frac{EI}{W^2} = K \eta \frac{D_x}{W^2} \quad (6)$$

where  $\eta = \underline{E}_t/\underline{E}$ ,  $\underline{E}$  being the elastic modulus and  $\underline{D}_x$  the Taber stiffness in the case of linerboard. It should be noted that  $\eta = \underline{E}_t/\underline{E}$  is a function of  $\underline{P}_{cr}$ . For a given material,  $\underline{E}_t$  may be evaluated from the compression stress-strain curve. A graph of  $\eta$  vs.  $\underline{P}_{cr}$  will appear, in general, as shown in Fig. 5. That is, for loads less than the proportional limit ( $\underline{P}_{pl}$ ),  $\underline{E}_t = \underline{E}$  and  $\eta = 1.0$ . Above  $\underline{P}_{pl}$ , the tangent modulus progressively decreases and  $\eta$  decreases.

Taking  $\underline{D}_x$  as the average Taber stiffness of the two facings of combined board and  $\underline{P}_{cr} = \underline{P}_{mx}$ , Equation (6) may be written as

$$\frac{P_{mx}}{\eta} = 2K \frac{D_x}{W^2} \quad (7)$$

and it is seen that calculation with Taber stiffness yields an estimate of  $\underline{P}_{mx}$  which differs from the true  $\underline{P}_{mx}$  by a factor  $1/\eta$ . In view of Fig. 5, it may

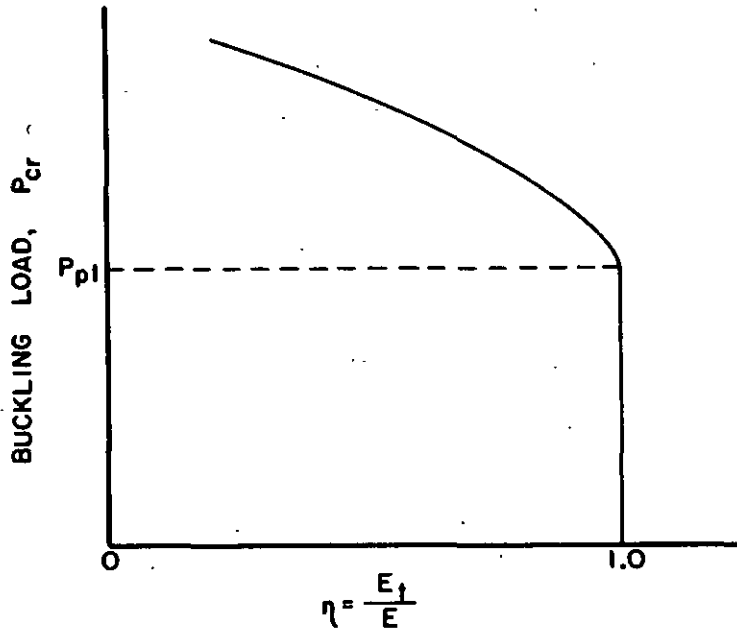


Figure 5. Illustrative Relationship Between Buckling Load  $P_{cr}$  and Tangent Modulus  $\underline{E}_t$  ( $\underline{E}$  = elastic modulus)

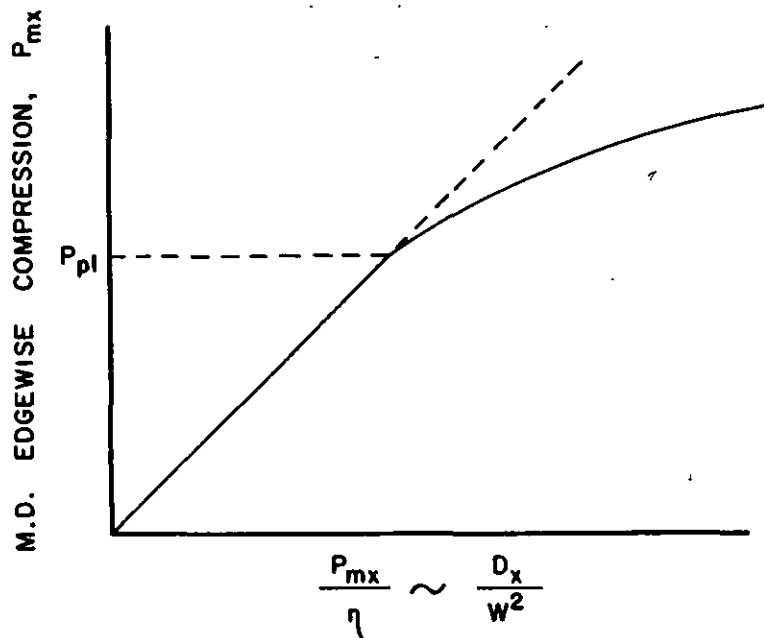


Figure 6. Illustrative Relationship Between Buckling Load and Elastic Buckling Parameter  $\frac{D_x}{W^2}$

be deduced that a graph of  $\frac{P_{\underline{mx}}}{\eta}$  vs. the "fictitious" buckling load  $\frac{P_{\underline{mx}}}{\eta}$  will appear as shown in Fig. 6. The relationship is a straight line of slope 1.0 up to the proportional limit. At higher (inelastic) loads the relationship is curvilinear in the sense shown, with the exact shape depending on the function  $\eta = \frac{E_t}{E}$  for the given material, as illustrated schematically in Fig. 5. As a practical matter one may reasonably approximate the entire curve of Fig. 6 by a curvilinear function (say, a power function) although strictly it is a straight line below the proportional limit. Although the curve illustrated in Fig. 6 is specific to a given material, it is clear that all conventional linerboards will exhibit curves of this general shape.

It may be noted that the variables graphed in Fig. 6 are the same as were plotted in Fig. 3 in the main body of the report for the 45 samples of corrugated board. Thus, it may be seen that there are theoretical grounds for fitting a power function (concave to the horizontal axis) to the data for the collection of samples given in Fig. 3.

It should be remarked that the relationship given by Fig. 6 represents a conventional procedure for calculating the inelastic buckling load for a column of a specific material. From the experimental stress-strain curve, Fig. 5 and hence Fig. 6 may be constructed. The latter curve may be entered on the horizontal axis for a particular cross section and column length, and the inelastic buckling load may be read out on the vertical axis. The procedure is laborious, however, because of the required determination of  $\frac{E_t}{E}$  of the material.

